

## Pinning of size-selected gold and nickel nanoclusters on graphite

M. Di Vece, S. Palomba, and R. E. Palmer

*Nanoscale Physics Research Laboratory, School of Physics and Astronomy, The University of Birmingham, Edgbaston, Birmingham B15 2TT, United Kingdom*

(Received 26 April 2005; published 26 August 2005)

Size-selected gold and nickel nanoclusters are of interest from an electronic, catalytic, and biological point of view. These applications require the deposition of the clusters on a surface, and a key challenge is to retain the cluster size. Here controlled energy impact is used to immobilize the size-selected clusters on the graphite surface at room temperature. The threshold energy for pinning of ionized  $\text{Au}_N$  ( $N=20-100$ ) and  $\text{Ni}_N$  ( $N=10-300$ ) clusters, over the impact energy range 350–2000 eV, is shown by scanning tunneling microscopy to scale with the cluster mass. This behavior is consistent with a previous study of silver clusters and demonstrates the more general applicability of the cluster pinning model.

DOI: [10.1103/PhysRevB.72.073407](https://doi.org/10.1103/PhysRevB.72.073407)

PACS number(s): 61.46.+w, 79.20.Rf, 68.37.Ef

### INTRODUCTION

Size-selected nanoclusters represent model systems for exploring the fascinating properties of nanometer-scale objects, which are considerably different from their macroscale counterparts. Besides the major interest in the properties of clusters from a fundamental point of view,<sup>1</sup> the utilization of these new, exotic materials forms a intriguing technological challenge.<sup>1,2</sup> One way to study and exploit the distinctive properties of nanoclusters is by deposition on smooth surfaces. Different deposition energy regimes can be distinguished for nanocluster deposition, resulting in different interaction processes between the cluster and substrate. In general, nanoclusters can be scattered, fragmented, soft-landed, deformed, implanted, or pinned on a surface.<sup>3</sup> Cluster pinning<sup>6</sup> is a process by which the incident cluster is immobilized at the point of impact on the surface, leading to the creation of monodispersed arrays of size-selected clusters which are stable at room temperature and even above.<sup>4</sup> One example of the utility of such cluster films is given by demonstrating the surface immobilization of proteins on clusters.<sup>5</sup>

The pinning of size-selected silver clusters deposited on graphite as established by Carroll *et al.*<sup>6</sup> revealed a linear relation between the pinning threshold energy and the cluster size. Pinning was proposed to occur when the cluster had sufficient energy to displace a carbon atom from a surface lattice site. A question arising is then whether this pinning energy behavior versus size is valid for different cluster materials. Gold is particularly interesting because of its application in electronics and catalysis as well as the interaction with protein (via cysteine residues). Nickel has similar applications in magnetism, catalysis (e.g., growth of carbon nanotubes), and protein interactions (via histidine residues). In this work we therefore investigate the pinning of gold and nickel clusters on the graphite surface as a function of impact energy and size.

### EXPERIMENT

The size-selected gold and nickel clusters are produced in a magnetron sputtering, gas aggregation cluster source<sup>7-9</sup> and

mass selected ( $M/\Delta M \sim 25$ ) by a novel lateral time-of-flight mass filter.<sup>10</sup> The following cluster sizes were explored:  $\text{Au}_x$  ( $x=20, 40, 55, 70, 100$ ) and  $\text{Ni}_y$  ( $y=10, 20, 50, 100, 200, 250, 300$ ). The range of investigated impact energies was for gold 0.2–1.8 keV and 0.05–2.5 keV for the nickel clusters. The clusters were deposited in high vacuum on graphite and imaged in the ambient with a scanning tunneling microscope (STM) (DME, Rasterscope 4000); the employed imaging parameters were a sample bias voltage of 300 mV and a tunnelling current of 0.1 nA, in accordance with the work of Carroll *et al.*<sup>6</sup> The Pt/Ir tips were mechanically cut. The height distribution of the clusters in the STM images was analyzed with a scanning probe image processor (SPIP, Image Metrology) program.

### RESULTS AND DISCUSSION

The experimental pinning threshold energy was determined for both the gold and nickel clusters by measuring the density of the clusters observed on the graphite surface; specifically, we determine the ratio of the number of clusters detected by the STM to the number of clusters incident on the same surface area, derived from the integrated deposition current.<sup>6</sup>

An STM image of  $\text{Au}_{70}$  clusters deposited and pinned on graphite is shown in Fig. 1(a) together with a histogram of the measured cluster height for deposition of  $\text{Au}_{70}$  at 1.20 keV in Fig. 1(b). Note that the height distribution includes differences in the electronic structure of the cluster and substrate. The  $\text{Ni}_{250}$  cluster height distribution pinned on graphite with a deposition energy of 1.80 keV is presented in Fig. 1(c).

A typical graph of cluster density as a function of deposition energy is shown in Fig. 2. It is clear that at the lower energies the density is close to zero, while in a certain range of impact energies the density increases quite sharply to reach a plateau value. The midpoint of the transition from approximately zero to maximum density defines the pinning threshold energy in accordance with the procedure of Carroll *et al.*<sup>6</sup> in their demonstration of the self-pinning of  $\text{Ag}_N$  clusters on graphite. Reference 6 also presented a simple analyti-

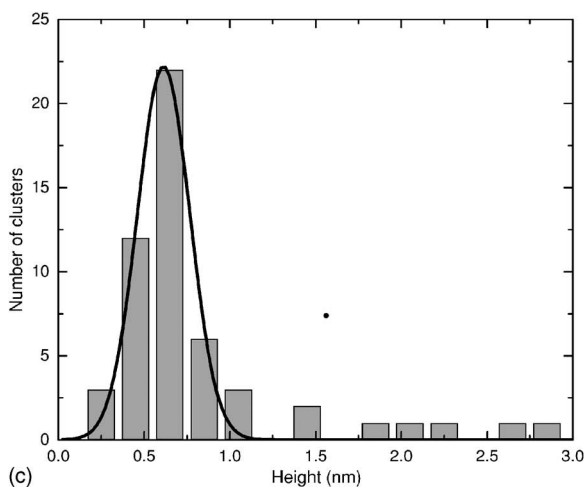
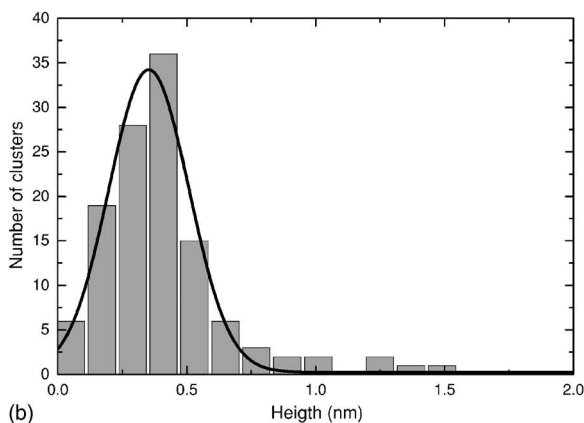
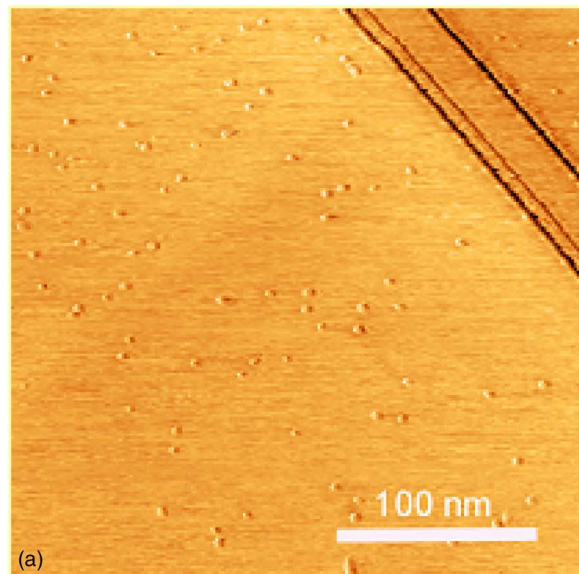


FIG. 1. (Color online) (a) An STM image of Au<sub>70</sub> clusters pinned on graphite. Typical examples of the cluster height distribution of Au<sub>70</sub> deposited at 1.20 keV (b) and Ni<sub>250</sub> deposited at 1.80 keV (c). The height distribution is fitted by a Gaussian of which the center defines the height.

cal model to complement the detailed experiments and molecular dynamics simulation, which identified the pinning mechanism. The analytical model yielded the result

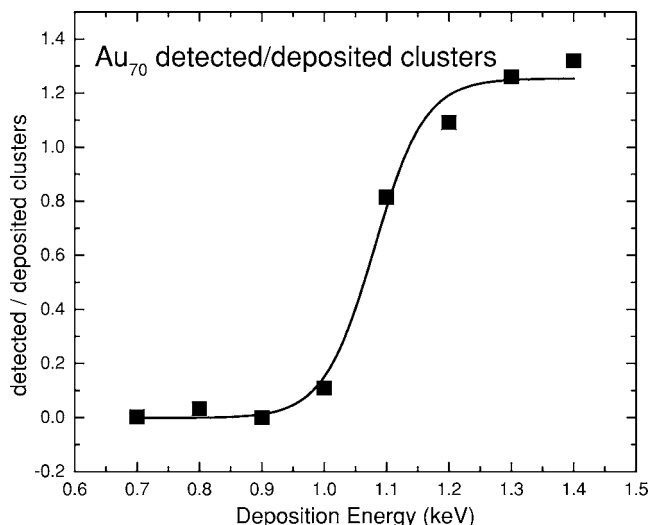


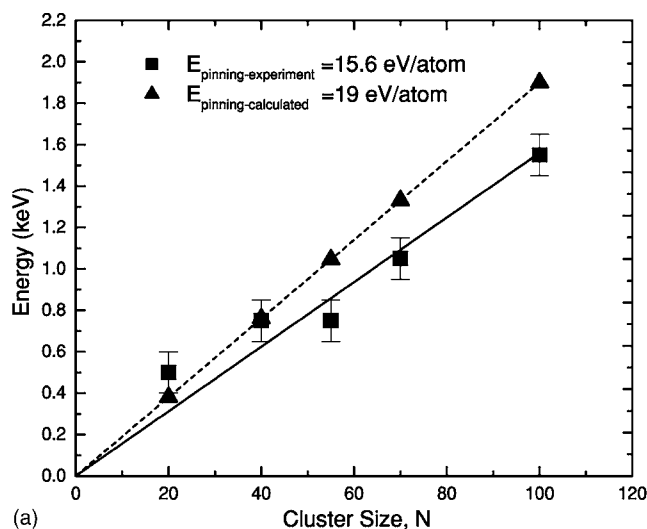
FIG. 2. The cluster density as a function of deposition energy for Au<sub>70</sub><sup>+</sup> clusters impact on graphite. The midpoint between the two plateaus defines the pinning threshold energy.

$$E_{\text{pinning}} = NM_{\text{element}} \frac{E_T}{4M_C}, \quad (1)$$

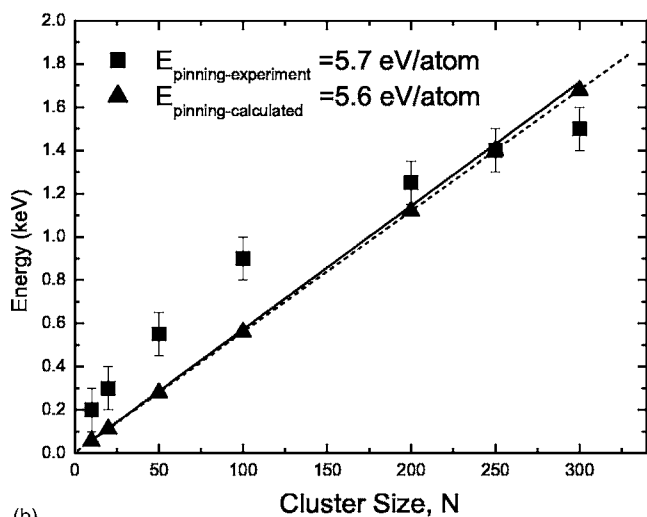
in which  $E_{\text{pinning}}$  is the kinetic energy to pin the cluster,  $N$  is the number of atoms in the cluster,  $M_{\text{element}}$  and  $M_C$  are the mass of the cluster material and carbon, respectively, and  $E_T$  is the transferred energy to displace a carbon atom. This relation was derived from the conservation of energy and momentum in a binary elastic collision. The generality of this simple picture is tested in Fig. 3 by extrapolating the pinning model to gold and nickel just by changing the atomic mass of the cluster atoms in Eq. (1).

Below the pinning threshold, we do not observe clusters in the STM images. In previous cluster deposition studies, gold and silver cluster islands were observed on graphite.<sup>11,12</sup> The formation of these islands is explained by a high mobility of the gold clusters on the graphite surface. In the present study a much lower cluster coverage is used. Inspection of the STM figures indicates at least an order of magnitude higher cluster density in the work of Ref. 13. We suggest that at low density the mobile clusters diffuse to defect sites such as step edges and/or that isolated clusters on the terraces are easily displaced by the STM tip.

Figure 3 presents the experimentally determined pinning threshold energies as a function of cluster size. The values for gold in Fig. 3(a) (squares) show a dependence on the cluster size, which is close to linear as previously found for silver clusters.<sup>6</sup> Fitting the results (including the origin of the graph) with a best straight line yields a pinning energy of 15.5 eV/atom. This value deviates from the 19 eV expected based on a simple extrapolation of the silver results [triangles in Fig. 3(a)]. The estimated error in these values, mainly determined from the step curves illustrated in Fig. 2, is of order 10% for both this study and the previous silver results.<sup>6</sup> The modest difference of 3.5 eV between the experimental and extrapolated values for the pinning of the gold clusters suggests that a similar pinning mechanism applies for both



(a)



(b)

FIG. 3. The pinning threshold energies as a function of size for (a) gold and (b) nickel clusters as obtained by experiment (■) and derived from previous silver results (▲) in each case.

gold and silver clusters. The somewhat reduced kinetic energy for the gold cluster pinning might arise from the larger binding energy of a gold adatom or dimer to graphite, which is calculated to be twice as much as for silver on graphite.<sup>14,15</sup> Since

the metal-C interaction has an influence on the defect formation process and on the binding of peripheral cluster atoms to the surface, it seems reasonable that a shorter metal-C bond should correlate with a reduction in the kinetic energy needed for pinning.

The experimental nickel cluster pinning energies as a function of size are shown in Fig. 3(b) (squares). Fitting with a straight line through the origin results in a slope corresponding to a pinning energy of 5.7 eV/atom. This is notably close to the extrapolated value of 5.6 eV/atom based on the silver pinning model [triangles in Fig. 3(b)]. However, in this case it is apparent that the experimental pinning values deviate significantly from the straight line. The values for the small clusters are overly large, while the largest cluster has an overly small pinning energy. The deviation exceeds the margin of the estimated experimental errors and implies that the simple binary collision model is only a rough approximation in the case of nickel. Calculations of the interaction between the nickel clusters and the graphite substrate, including the cluster  $d$  bands, might cast further light on the interaction. Of course, the experimental results still stand as a recipe for the production of films of pinned clusters of different sizes.

## CONCLUSIONS

The phenomenon of cluster pinning has been demonstrated for gold and nickel clusters on the graphite surface. The corresponding pinning threshold energies have been obtained for  $Au_N$  up to  $N=100$  and  $Ni_N$  up to  $N=300$ . In the case of the gold clusters, the dependence of the pinning energy on the cluster size is approximately linear and only about 20% below the values extrapolated from the original demonstration of pinning with silver clusters. The mean pinning energy per atom for nickel is close to the extrapolated silver values, but the observed dependence on cluster size is markedly nonlinear. The results obtained allow a precise preparation of stable films of size-selected gold and nickel clusters for a diverse range of applications.

## ACKNOWLEDGMENT

The authors thank the EU Nanocluster network and EPSRC for financial support.

<sup>1</sup>C. Binns, Surf. Sci. Rep. **44**, 1 (2001).

<sup>2</sup>R. E. Palmer, S. Pratontep, and H.-G. Boyen, Nat. Mater. **2**, 443 (2003).

<sup>3</sup>H. Hsieh, R. S. Averback, H. Sellers, and C. P. Flynn, Phys. Rev. B **45**, 4417 (1992).

<sup>4</sup>F. Yin, C. Xirouchaki, Q. Guo, and R. E. Palmer, Adv. Mater. (Weinheim, Ger.) **17**, 6 (2005).

<sup>5</sup>C. Leung, C. Xirouchaki, N. Berovic, and R. E. Palmer, Adv. Mater. (Weinheim, Ger.) **16**, 3,223 (2004).

<sup>6</sup>S. J. Carroll, S. Pratontep, M. Streun, R. E. Palmer, S. Hobday,

and R. Smith, J. Chem. Phys. **113**, 7723 (2000).

<sup>7</sup>I. M. Goldby, L. Kuipers, B. von Issendorff, and R. E. Palmer, Rev. Sci. Instrum. **68**, 3327 (1997).

<sup>8</sup>C. Xirouchaki and R. E. Palmer, Philos. Trans. R. Soc. London, Ser. A **362**, 117 (2004).

<sup>9</sup>S. Pratontep, S. J. Carroll, C. Xirouchaki, M. Streun, and R. E. Palmer, Rev. Sci. Instrum. **76**, 045103 (2005).

<sup>10</sup>B. von Issendorff and R. E. Palmer, Rev. Sci. Instrum. **70**, 4497 (1999).

<sup>11</sup>L. Bardotti, P. Jensen, A. Hoareau, M. Treilleux, B. Cabaud, A.

- Perez, and F. Cadete, Surf. Sci. **367**, 276 (1996).
- <sup>12</sup>M.-D. Schaffner, J.-F. Jeanneret, F. Patthey, and W.-D. Schneider, J. Phys. D **31**, 3177 (1998).
- <sup>13</sup>N. Vandamme, E. Janssens, F. Vanhoutte, P. Lievens, and C. Van Heasendonck, J. Phys.: Condens. Matter **15**, S2983 (2003).
- <sup>14</sup>G. M. Wang, J. J. BelBruno, S. D. Kenny, and R. Smith, Phys. Rev. B **69**, 195412 (2004).
- <sup>15</sup>G. M. Wang, J. J. Belbruno, S. D. Kenny, and R. Smith, Surf. Sci. **541**, 91 (2003).